JOURNAL GEOLOGICAL SOCIETY OF INDIA
Vol.82, August 2013, pp.107-120

Integrated Mineral Magnetic and Lithologic Studies to Delineate Dynamic Modes of Depositional Conditions in the Leh Valley Basin, Ladakh Himalaya, India

S. J. SANGODE[1], SUMAN RAWAT[2], D. C. MESHRAM[1], N. R. PHADTARE[2] and N. SURESH[2]
[1]Department of Geology, University of Pune, Pune - 411 007
[2]Wadia Institute of Himalayan Geology, Dehradun - 248 001
Email: sangode@unipune.ac.in, suman@wihg.res.in, dcmeshram@unipune.ac.in, phadtarenr@wihg.res.in, suresh_n@wihg.res.in

Abstract: We present here lithofacies and mineral magnetic results from a ~50 m thick composite record of fluvial, lacustrine and aeolian facies within the Leh valley basin of Indus River in Ladakh Himalaya. Mineral magnetic studies decipher interplay of two contrasting sediment sources *viz.*, the unimodal ferrimagnetic source derived from Ladakh batholithic glacial domain and mixed ferri- to antiferromagnetic source derived from Indus sedimentary sequence. The lithofacies variability expresses dynamic changes in the depositional regimes controlled by base level fluctuations that are governed by the interaction of basin fill conditions and the response to Late Quaternary climatic perturbations.
A three stage evolution of the Leh valley basin is proposed after comparison to other characteristic lithofacies changes within the valley as: *(I)* the basin under-fill conditions marked by fluvial and fluvio-lacustrine phase till ~24m (~64 Ka OSL age) above modern base level followed by *(II)* predominantly varved, glacio-lacustrine, basin overfill phase till 38m (~28 Ka) gradually passing into an aeolian phase; and *(III)* basin incision that began at the earliest Holocene warming. Advancement and retreat of glaciers from the transverse valleys, attributed to climatic oscillations, appears to have greatly controlled the basin-fill conditions in the Leh valley. The present approach demonstrates its larger scope in recording the Late Quaternary response of individual valley basins to delineate local and regional attributes of climate change in the Himalayan and Karakoram region.

Keywords: Lithofacies, Mineral Magnetism, Quaternary climate, Himalaya.

INTRODUCTION

Late Quaternary sedimentation in the Himalayan region is primarily governed by climatic oscillations from glacial to interglacial cycles (Shroder and Higgins 1989; Owen et al 1998; Benn and Owen 2002; Bookhagen et al 2005). A combination of varied orographic and climatic factors resulted in contrasting glacial patterns across the Himalayan and Karakoram mountain belt (Owen et al. 2005, 2009). Systematic documentation and correlation of various sedimentary units across the de-glaciated valleys is, therefore, crucial to identify regional climatic and/or tectonic changes during the Late Quaternary period (Mitchell et al. 1999; Owen et al. 2009; Sangode and Gupta, 2010). This clearly demands a valley basin approach based on integrated lithologic and instrumental methods in order to define the sedimentary units and relate them locally or regionally.

The Leh, Nimu, Basgo, Nubra, Nyoma and Tangtse are some of the broad open valley basins in the Ladakh and Karakoram Himalaya preserving thick records of glacial-paraglacial, fluvial and lacustrine conditions (e.g., Burgisser et al. 1982; Fort et al. 1989; Sangode and Bagati, 1995; Kotlia et al. 1997; Owen et al. 1998; Shukla et al. 2002; Phartiyal et al. 2005; Sangode et al. 2011; Sant et al. 2011a, b). Amongst these, the Leh valley appears to have preserved some of the oldest records of glacial stages in the Himalaya-Karakoram and Tibetan region (Owen et al. 2006). Further, the sediment profile at Spituk in the Leh valley seems to represent one of the longest continuous records of Late Pleistocene-Holocene sedimentation (Phartiyal et al. 2005; Sangode et al. 2011; Sant et al. 2011a, b). We, therefore, present here an integrated mineral magnetic and lithofacies approach aided by Optically Stimulated Luminescence (OSL) chronology on the Spituk section and its broad correlation with other characteristic lithofacies changes across the valley.

0016-7622/2013-82-2-107/$ 1.00 © GEOL. SOC. INDIA

LATE QUATERNARY SEDIMENTATION IN THE LEH VALLEY BASIN

The Leh valley is an elongated (longitudinal) and presently misfit valley basin of the Indus River (Fig. 1). It also characterizes a morphometric asymmetry of the basin (described in Jamieson et al. 2004) as a result of litho-tectonic divide in the form of folded Indus Molasse in left flank and the Ladakh batholith in the right flank. The left bank is extensively aproned by the paraglacial fans (marked *Pf* in Fig. 2) overlapped at places by younger moraines (e.g., *M* in Fig. 2) including sporadic deposits of outwash gravels. These paraglacial fans are explained as the records of terminal 'Indus Stage' glaciation (>430 Ka) by Owen et al., (2006). These fan terraces also show sharp toe cutting due to the transversely flowing Indus River (See Fig. 3a). Majority of the exposed vertical profiles along the Indus River show sheet geometry without any visible fan coalescence. This is due to rapid drop in fan gradient from mountainous fronts to the broad open valley basin and their coeval and episodic nature (See Fig. 2).

The right bank flanks the Ladakh batholithic range, and shows some of the major transverse valleys (marked *Tv/1….Tv/8* in Fig. 2) with moraines visibly approaching the valley floor, particularly in the northern end of the Leh valley basin. Some of these transverse valleys also show broad triangular shape geometry, opening into the main Leh valley preserving remnant glacial outwash and lag deposits and are described as amphitheater valleys by Sant et al. (2011b). In the upstream region (southern tip of the valley), the right bank also shows dynamic interaction marked by litho-facies cross-cut relation and scouring of the fluvial, lacustrine and glacial phases (*e.g.,* Fig. 3c). The clast supported, rounded to sub-rounded gravel deposits of Paleo-Indus are overlapped and scoured,at places, by the younger, transverse moraine deposits. At Shey in the central part of the right bank, a terminal moraine deposit is overlain by thick aeolian dune facies (*e.g.,* Fig. 3d and described later in detail). The cross profiles (*a-a'* to *h-h'*, in Fig. 2) depicts the geometry of the valley basin. The Quaternary units shown are broad extrapolation from surface observations. All these profiles show trough shaped valleys depicting their glacial origin.

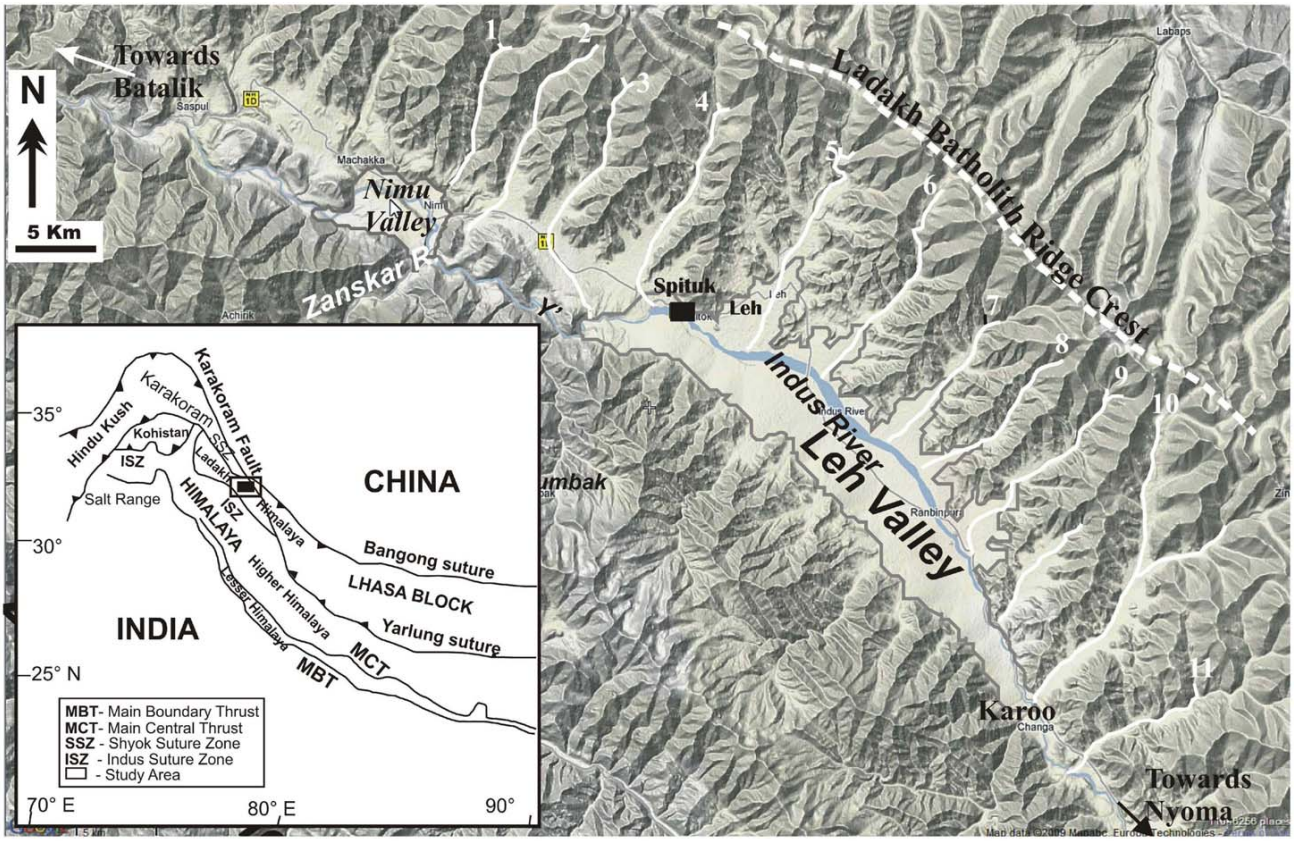

Fig.1. The Google Earth image depicting the study area of the Leh valley and surrounding. The prominent transverse streams are demarcated as 1 to 11 [1: Nimu tokpo, 2: Umlah fu, 3: Taru, 4: Fyang fu, 5: Khardung (Tangpo), 6: Sabu, 7: Stakma, 8: Thikse, 9: Nang, 10: Chemre, 11: Igu], some of which are inferred to play significant role in the basin fill conditions in the Leh valley basin. The inset shows the regional litho-tectonic configuration of the Himalaya and Karakorum ranges.

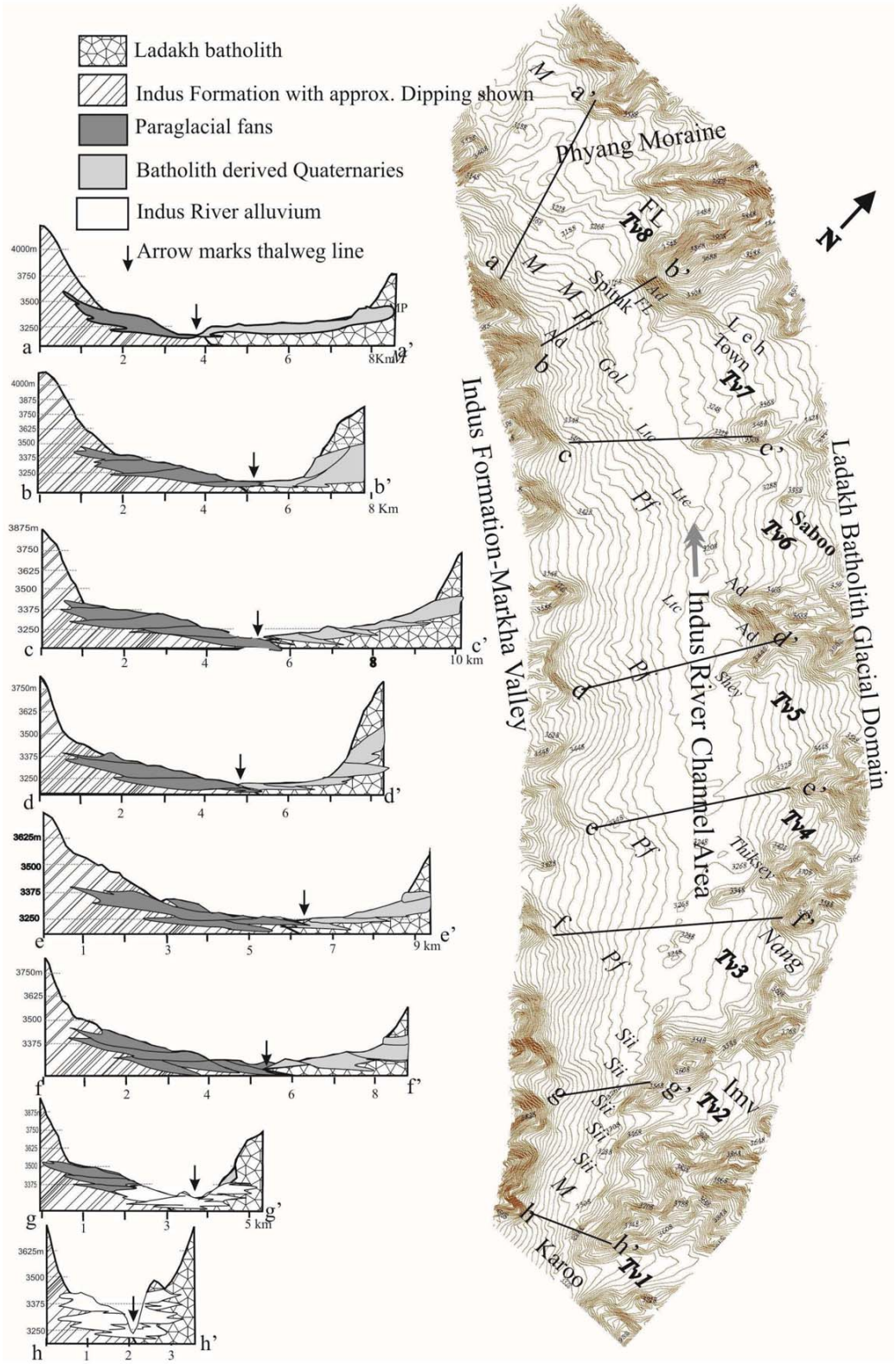

Fig.2. Generalized geomorphic map of the Leh valley including eight cross sections (named *a-a', b-b'…..h-h'*). *tv1…tv8*: the transverse valleys, also called amphitheater valleys (in Sant et al., 2011a), *Pf*: Paraglacial fans are the older formative surfaces in the valley and show toe cutting marked by the drop in contour (*Ltc*: level of toe cutting), *M*: Indicates remnant moraines, *Imv*: intermontane valley, *FL*: fluvio-lacustrine deposits, *Gol*: glacial outwash lacustrine deposits, *Ad*: Aeolian dune deposits, *Sii:* Scourings. Contours from Global Mapper 12

Fig.3. (a) Panoramic view looking towards the left bank, displays the arrangement of paraglacial fans derived from the Indus molasses ranges, **(b)** panoramic view of the extensive fluvio-lacustrine deposits truncated and covered by younger moraine deposits in the northernmost (downstream) part of the valley, **(c)** Scouring of the lacustrine phase by younger moraines seen in the southern i.e., upstream part of the valley, **(d)** a sequence of moraine deposits followed by aeolian dune and then glacial outwash conditions occurring near Shey in the central part of the valley.

The valley floor is notably broad in Spituk, Leh and Saboo areas preserving remnant fluvio-lacustrine deposits more prominently near the right bank, and the gravelly braided fluvial deposits in the central part. The fluvio-lacustrine deposits are well exposed linearly all along the valley margin in the right bank near Airport, Spituk monastery and the Army Check Post at the National Highway (marked NH 1D in Fig. 1). The NH 1D deposits are particularly extensive, displaying thick (>30 m) fluvio-lacustrine sedimentation ending with aeolian phase at the top. The fluvio-lacustrine facies are of massive nature and mainly contain siltstone, mudstone and channel lag deposits in the vertical profile. The channel deposits show pebble imbrications showing the average flow direction of modern Indus River. We observed that these pebbly layers of fluvial deposits occur at various stratigraphic levels up to 20-30 m from the modern base level (i.e., T_0 surface of the modern Indus River).

The northern tip of the valley outlet shows moraine deposits and their recycled sediments sourced from Phyang transverse valley shifting the Indus River towards left bank and into the sinuous gorge as explained above. The moraines in the northern (downstream) part of the valley appear to have episodically produced significant damming effects for the Indus River as reported by Sangode et al. (2011).

FIELD AND LABORATORY METHODS

Field documentation includes noting the routine sediment characters like fining (/coarsening) upwards cycles, contact relations of sedimentary units, clast compositions, color variation, approximate varve frequency and the deduced depositional environments (See Table 1). Thicknesses and heights of each unit are measured from the T_0 surface as the reference level. For mineral magnetism, about 500 gm of sample collected from each horizon in the field, was reduced

to 10 gm by coning and quartering in the laboratory. This sample (/specimen) was then tightly packed in a standard non-magnetic styrene pots and necessary corrections are made for weight and susceptibility of the bottle. The initial susceptibility was computed by averaging out the susceptibilities of six orthogonal directions for each specimen in Bartington's MS-2B sensor for low and high frequency (0.465 and 4.65 kHz) fields. Each specimen was then subjected to Isothermal Remanant Magnetization (IRM) by sequential exposure to the incremental DC fields up to 1200 mT at the intervals of 20/50/100/200 mT in an automated and calibrated solenoid based instrument IM 10-30 Impulse Magnetizer of ASC Scientific (USA). Specimens were then exposed to back fields in the reverse direction up to 700 mT at various close intervals. The remanant magnetization for each step was measured using Minispin Rock Magnetometer of Molspin, (UK). Anhysteretic Remanant Magnetization (ARM) was grown by a constant biasing field of 0.1 mT superimposed over a peak alternating field (a.f.) of 100mT decaying at the rates of 0.01 mT per cycle using Molspin a.f. demagnetizer with ARM facility. All the magnetic analysis was conducted at the Rock Magnetic laboratory of Wadia Institute of Himalayan Geology (Dehradun). Finally, the following room temperature based rock magnetic parameters were deduced for the mineral magnetic inferences presented in the later sections.

K_{lf} and χ_{lf}: initial magnetic susceptibility [volume (K_{lf}) and mass (χ_{lf}) based values] taken as bulk representation of the ferrimagnetic. ***χ_{fd}:*** frequency-dependence of susceptibility to estimate the ferrimagnetic grain size in restricted range of finer/superparamagnetic (SP) domains. ***χ_{ARM}:*** susceptibility of anhysteretic remanent magnetization that varies with concentration of particles with stable remanence reflecting the domain size called Single Domain (SD). ***SIRM:*** saturation isothermal remanent magnetization which reflects the concentration of remanence carrying minerals. ***SIRM/χ_{lf}:*** a ratio sensitive to mineralogical and grain size variations amongst ferri- and antiferromagnetic oxides. ***Hcr:*** remanence coercivity representing the demagnetizing field required to reduce the SIRM to zero. ***S-Ratio*** (= $IRM_{-100mT}/SIRM_{1000mT}$): a ratio to provide a relative measure of high or low coercivity minerals within its SIRM. The higher negative values of S-ratio indicates presence of multi domain (MD) magnetite of detrital origin, whereas the lower negative values can infer SD magnetites and low positive values suggest mixtures of magnetite and hematite, with higher positive values suggesting the presence of hematite. More details on the rock magnetic aspects, mineral magnetic parameters and methods are available in the widely referred texts (Collinson, 1987; Dunlop and Ozdemir, 1997; Thompson and Oldfield, 1986; Evans and Heller, 2003).

Luminescence Dating

Three samples were selected for optically stimulated luminescence (OSL) dating considering their significance in litho-section. The samples were prepared in dark room under subdued red light conditions. The size fraction in the range of 90-125 µm was extracted after basic treatment of 1 N HCl and 30% H_2O_2 and quartz grains were extracted using heavy liquid separation (density 2.65 gm/cc), then etched in 48% HF acid for 80 minute, washed with HCL and distilled water, and finally re-sieved. Small aliquot (monolayer of 3 mm diameter) of the treated quartz was mounted on stainless steel disc and analyzed by Single Aliquot Regeneration (SAR) technique (Murray and Wintle, 2000). The OSL measurements were carried out in an automated TL/DA 20 Riso reader with blue light emitting diodes (blue LED's) as stimulation source. Total 30-35 aliquots were prepared for each sample and each aliquot was subjected to a series of cycles of measurement to obtain the equivalent dose (ED) as described in Murray and Wintle (2000). A preheat of 240°C for 10 sec and a cut-heat of 160°C were applied, and the luminescence signal was measured for 40 sec. The equivalent doses (ED) were calculated using initial integral (0.8 sec) of the luminescence signal by Duller's software (Duller, 2008). For the dose rate estimation; U, Th and K concentration in the sediments were measured by XRF. The percentage of moisture content was calculated as dry weight by heating the sediments to 100 °C in a laboratory oven. Finally the ages were calculated using Grun's software.

DEPOSITIONAL ENVIRONMENTS

The 50m thick measured sequence at Spituk is sub-divided into 51 units based on the characteristic sedimentologic attributes (e.g., marked in photo figures 3 to 6) for lithofacies reconstruction (Fig. 4). The detailed account of lithology of each unit is given in Table 1. The temporal controls over depositional environments are tentatively obtained by using the age interpolation from the 3 OSL as shown in Fig.7. The bounding surfaces for each set of facies (or units) inferring the depositional environments can be time transgressive. This can occur due to lateral litho-facies variations resulting from the variable response times of sedimentation across the basin because of the asymmetric basin geometry of the Leh valley.

Table 1. An account of sedimentologic attributes for the studied lithosection of Spituk near Leh. Inferred depositional environments are given in italics.

Unit	Description
1	In order to expose the base below modern T_0 surface, a 1.5m dip trench was opened and assigned as unit '0', which shows fining upward grey sand with fine bedding laminations. The Unit 1 starts from the T_0 surface and comprises ~15 cm thick yellowish grey fining upward cycle grading from fine sand to silty mud (See figs. 4 and 5). There is a fine calcrete layer (~2-3 mm) in the middle part of this unit. *Depositional Environments: Fluvial.*
2	~185 cm thick sand dominated interval of relatively darker, medium to coarse grained sands, thinly laminated with mud and grading into medium to fine grained sand with ripple laminations at the top. This entire unit shows convolute bedding with hydroplastic flows (PCD's) within the sand and yellow mud layers. The intensity of deformation increases towards the top of the unit. *Fluvio-lacustrine.*
3	The lower part of this unit shows medium to coarse grained sand layer varying in thickness from 5 to 10 cm showing PCD at the top. The PCD is laterally traceable to a distance of ~40m for the entire length of the outcrop. It shows a well sorted, grey, but intensely liquefied silt injected into the upper unit of medium to coarse grained sand. *Fluvio-lacustrine.*
4	20 to 35 cm thick, coarse grained, fining upward sand layer containing thin limonitic layers and 3-5 mm angular mud clasts. It shows liquefactions injected from the underlying layer (see unit 3 above). *Fluvio-lacustrine.*
5	~125 cm thick fining-up massive sand, grading upwards into silt. *Fluvial.*
6	~10 cm thick fine silt with thin lenticular laminations of mud overlain by a 5 cm thick fine silty sand layer, followed by 12 cm thick fine sand with liquefied mud layer. *Fluvio-lacustrine.*
7	~35 cm thick light yellowish grey, massive mudstone, laterally transitional into silt and sand, showing ball and pillow structures at the top. *Lacustrine.*
8	Lower part of this unit shows a 27 cm thick mudstone package of thinly laminated (0.5 to 2 cm each) mud layers. This is followed by 32 cm thick massive mudstone showing PCDs, a 30 cm thick laminated mudstone and then 38 cm thick massive mudstones. The greater thickness and lateral continuity of this mud dominated unit probably indicates the first extensive lacustrine phase in this basin. *Lacustrine.*
9	This unit shows 38 cm thick laminated silty mudstone followed by 40 cm thick massive sandstone, 6 cm thick laminated mudstone and then 30 cm thick massive PCD bearing mudstone. *Fluvio-lacustrine.*
10	This unit consists of 17 cm thick, thinly laminated, interlayered sand and silt showing ripple marks. The symmetrical ripples indicate oscillatory nature of deposition under shallow water conditions (See fig. 5). *Fluvio-lacustrine.*
11	~15 cm thick laminated siltstone unit grading upwards into light cream colored mudstone. The upper part becomes grayish, fine, silty sand and shows thin laminations. *Fluvio-lacustrine.*
12	Basal part of this unit shows 3.5 cm thick siltstone showing interference ripples followed by 2 cm thick massive mudstone and 24 cm thick fine sand layer with complex convolute structures (Seen in fig. 5). Top of this unit shows liquefaction injecting into upper layer. *Fluvio-lacustrine.*
13	~37 cm thick fine grained and thinly laminated sandstone layer containing course grained, laterally pinching-out sand layers in the middle part. *Fluvial.*
14	~50 cm thick, monotonous thinly laminated mudstone. *Lacustrine*
15	~75 cm thick fining upward sand with alternation of coarse and medium grained sands. The coarse sand contains well imbricated, rounded to sub-rounded pebbles of Indus clasts. *Fluvial.*
16	~105 cm thick unit of dark grey, medium grained sands of massive nature. *Fluvial.*
17	~20 cm thick coarse grained sandstone inter-layered with mud showing liquefaction. *Fluvial to Fluvio-lacustrine.*
18	~22 cm thick fining upward cycle of course to medium grained sand with top showing liquefaction structures. *Fluvial.*
19	Lower part of this unit contains 60 cm thick massive sandstone with trough cross stratifications (paleoflow towards $N280^0$), and contains mud clasts. This is overlain by ~20 cm thick thinly laminated sand. *Fluvial.*
20	Lower part of this unit shows a massive yellowish-white, 100 cm thick mudstone scoured by pebble based coarse grained sandstone (laterally pinching out). The pebbles show imbrications of N230°-200°. This is followed by a 10-30 cm thick mudstone layer with abundant cut bank material of dark grey sandstone clasts (Fig. 5). *Fluvial, Fluvio-lacustrine.*
21	~ 140 cm thick coarse grained, stratified, fining upward sandstone. At the bottom it shows angular clasts of 1-2 cm including subordinate clasts of 5-6 cm of Indus molasse composition. The pebble imbrications in this unit show a paleoflow trend of N240°-250°. Towards the top it becomes limonitic with medium grained sandstone having an out-sized clast of Ladakh batholith of ~20x7 cm (otherwise the general clast composition is of Indus affinity). *Fluvial.*
22	~65 cm thick fining upward cycle of course to medium grained sandstone showing parallel laminations at the base and ripple laminations at the top. It contains rare clasts of 2-3 cm size of Indus molasse composition. The top of this unit shows convolute bedding. *Fluvial.*
23	~96 cm thick massive sand of fining upward nature. *Fluvial*
24	~20 cm thick medium to fine grained sandstone with lower part showing parallel laminations and the upper part is ripple laminated. *Fluvial.*
25	~88 cm thick fining upward cycle of medium to fine grained massive sandstone followed by 34 cm thick parallel laminated, medium to fine grained sandstone showing pseudo-nodules (fig. 6). *Fluvial.*
26	~90 cm thick, yellow colour massive mudstone. It shows two 2 to 4 cm thick layers of greenish grey mudstones separated by a 9 cm thick yellow mud layer. The greenish mudstone is faulted with 3 to 5 cm of throw and the trend of the fault is N330°. *Lacustrine.*
27	~30 cm thick light yellow colour massive mudstone followed by 1-2 cm thick olive green mudstones showing convolute bedding at the top. *Lacustrine.*

Table 1. Contd.

Unit	Description
28	~40 cm thick massive light yellow colour mudstone. This unit exposes a basement (granitic) rock structure. The mudstone also contains rare granite clasts (Fig. 6). *Lacustrine.*
29	Lower part of the unit shows 180 cm thick light grey massive siltstone. This is followed by 70 cm thick, thinly laminated clay overlain by 120 cm thick massive siltstone. *Lacustrine.*
30	~37 cm thick sequence of variegated mudstones (packages of limonitic, hematitic and some bluish grey colours of mudstone). Each package of thickness 5 to 6 cm shows a varve frequency of 4 to 10 varves per centimeter. The top part of this unit ends with limonitic varves. *Glacio-lacustrine.*
31	~66 cm thick unit of mudstone with mud packages of 5 to 6 cm thickness showing varve density varying from 3 to 4 per cm. Top of this unit is limonitic with fine layers of silt and fine sand. *Glacio-lacustrine.*
32	~67 cm thick unit of similar nature as that of above (units 30-31). However the thicknesses of mud packages have increased to 10 to 15 cm with 1 to 2 varves/cm frequency. It also contains a mud package of ~8 cm without any varves. *Glacio-lacustrine.*
33	~52 cm thick mudstone dominated unit of 7 to 8 cm thick packages containing 2 varves/cm. *Glacio-lacustrine.*
34	~88 cm thick unit of 5 to 8 cm thick mud packages. It includes one layer of 6 cm thick yellowish mud without varves. The average varve frequency is 2 to 3 per cm. *Glacio-lacustrine.*
35	~23 cm thick unit of laminated mudstone with two mudstone packages showing 1 to 2 varves per centimeter. *Glacio-lacustrine.*
36	~55 cm thick, coarse to fine grained, fining up cycle of sand, gradationally passing to silt. The lower part contains well stratified disc shaped clasts (up to 1 cm) of mixed nature (platy clasts of Indus molasse and rounded clasts of Ladakh granite/granodiorite). The pebbles show flow imbrications from N200° to 250°. *Fluvial.*
37	~85 cm thick, grey, fine sand with abundant cut bank material in the form of mud balls, mostly of lensoid to rounded shape. It also contains 35 to 70 cm thick sand lenses of coarse grained nature (Fig. 6). *Fluvial.*
38	This unit contains a 25 cm thick mudstone with variegated varves of grey, green, pink and light brown color followed by two units of 18 cm thick mudstones of similar nature. It further follows two ~18 cm thick and one 17 cm thick mud packages. The unit ends with a 9 cm thick maroon colored mudstone. *Glacio-lacustrine.*
39	In the lower part it shows a 60 cm thick package of variegated; grey, maroon and cream colored mudstones with about 6 packages of mudstones showing varve frequency of ~1 varve/cm. Top of this unit is terminated by few thin (1-2 mm) sandy layers. This is followed by another 60 cm thick variegated pink and grey colored mudstones with five packages of mudstones varying from 6 -12 cm in thickness maintaining 1 varve/cm with relatively diffused margins. This is followed by 17 cm thick mudstone separated by thin sand layers at the top and bottom, 65 cm of another cycle of mudstone with nine packages showing 1 varve/cm (top and base showing thin hematitic/limonitic sandy layers). Topmost part shows 60 cm thick unit of similar nature separated by thin layers of sand. *Glacio-lacustrine transitional with Aeolian.*
40	It shows a ~50 cm thick mudstone with 1 to 2 varves/cm, followed by 43 cm mudstone showing 7 packages of 2 to 3 varves/cm with increased varve symmetry. The varves are more prominent in this unit due to grain size difference rather than color. *Glacio-lacustrine transitional with Aeolian.*
41	This unit consists of 16 cycles of pink, grey, green and maroon mudstones (the cycle break up is 20, 20, 18, 20, 13, 23, 13, 8, 10, 15, 8, 7, 8, 6, 7, 25). The mudstones laminations are more prominent towards the top due to their separation by thin layer of sand (up to 1-2mm). *Glacio-lacustrine transitional with Aeolian.*
42	~45 cm thick sequence of alternate layers of fine sand, silt and mudstone. *Glacio-lacustrine transitional with Aeolian.*
43	Lower part of this unit shows 14 cm thick finely laminated mudstone with middle part relatively massive; and is followed by 16 cm thick silty layer with large number of climbing ripples of aeolian nature. This is followed by 6 cm thick finely laminated mudstone, the middle part of it being ferruginous and massive in nature, then 2 cm thick siltstone showing climbing ripples, 9 cm thinly laminated light brown mudstone with alternate silt layers and 15 cm thick massive ferruginous mudstone. *Glacio-lacustrine transitional with Aeolian.*
44	The lower part of this unit shows a 24 cm and 10cm thick massive siltstone followed by 12 cm thick cross-bedded siltstone. It follows a sequence of 19 cm thick massive mudstone, 3cm thick cross bedded siltstone, 16 cm thick fining upward sandstone grading into thinly laminated siltstone, 12 cm thick siltstone of similar cyclicity with top showing ripple laminations, 30 cm thick cycle of similar nature showing ripple laminations followed by a 40 cm massive siltstone with thin lamination at the top showing ripple laminations at places. *Aeolian*
45	~45 cm thick cross bedded aeolian sand with lower part showing 12 cm thick foresets and the top showing 15 cm thick foresets. *Aeolian.*
46	Lower part of the unit shows 17 cm thick ripple laminated siltstone followed by 70 cm thick siltstone whose upper and lower parts are planar laminated and the middle part is massive. *Aeolian*
47	~480 cm thick monotonous, grey colored, cross bedded sand of aeolian dune nature. *Aeolian.*
48	~180 cm thick package of thinly laminated, alternate ferruginous sand containing packages of 20 to 30 cm, separated by ferruginous clay layers. *Aeolian to Glacial Outwash*
49	~100 cm thick sandy unit with lensoid mud accumulation. *Aeolian with Glaciolacustrine episodes*
50	~70 cm thick coarse grained grey sand with fining upward cycle and cross bedding indicating fluvial (glacial outwash) conditions. *Stratified glacial outwash gravels.*
51	~250 cm thick cross bedded sandstone with two units (1 and 1.5 m each) of cross bedded sand at the base showing pebbly layer of 20 cm. *Stratified glacial outwash gravels.*

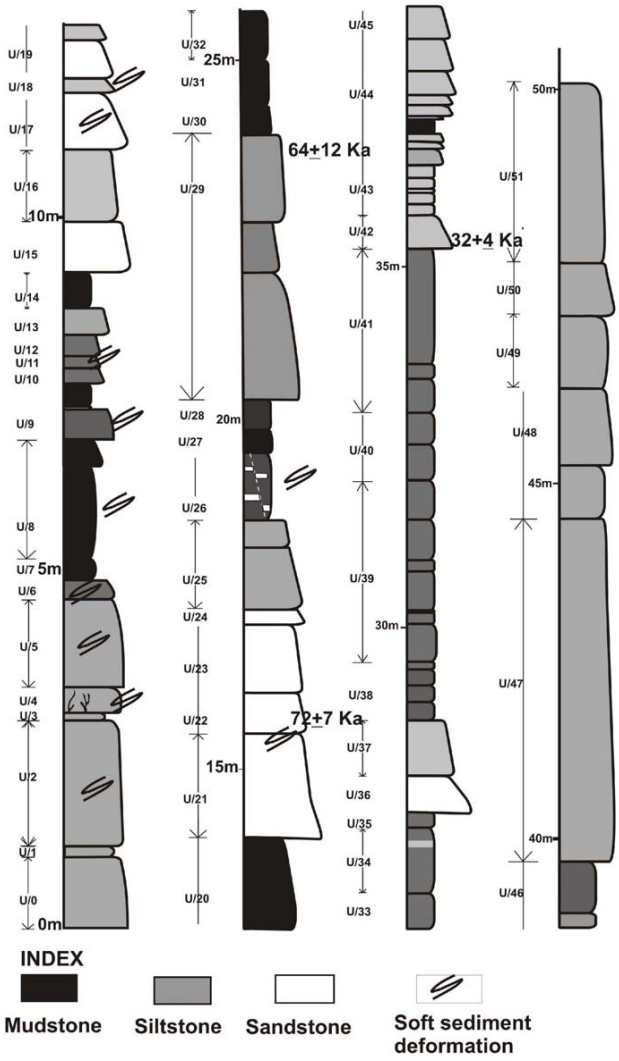

Fig.4. Litholog reconstruction for the Spituk-Leh section (sediment characters for each unit are given in Table 1 and the salient features discussed in text).

Therefore, we extrapolated the upper limits of the bar plot of each of the characteristic depositional facies till the last appearance of same depositional environment, assuming that the conditions (probably climate controlled) remained the same in the basin and elsewhere and no significant change-over in the depositional environments occurred during this period. This is justified in the absence of any detailed basin-wide control of time transgressive nature of lithofacies in the Leh valley. Apart from the fluvial environments, there are two major types of lacustrine facies; (i) with distinct varves and (ii) massive to poorly stratified, silty, lacustrine mudstones. The latter is associated with fluvial and fluvio-lacustrine conditions, whereas, the former indicate the glacial environments which began at about 24m above the T_0 surface in the studied section. The varved lake facies further passes gradually into aeolian facies. The extensive aeolian dune conditions are further followed by the stratified glacial outwash deposits.

Figure 7 depict an overall dominance of the fluvial and fluvio-lacustrine environments in the lower part (below 24 m) and the overall glacial dominating sequence above 24 m level. The 24 m level occurs above the OSL age of 64±12 Ka (see Table 1). The most prominent, thickest record of the gravelly deposit unit of Indus molasse clasts composition occur at unit 21 (~14 m level coinciding with the OSL age of ~73 Ka). Whereas, the last traces of such deposition is observed at unit 36 (~27.5 m) coinciding with the extrapolated age of ~32 Ka. These fining upward cycles of gravelly to fine sand units typically show planar bedding at the top and scouring at the bottom with lot of cut bank material. A combination of sedimentary structures such as cross bedding, trough cross stratifications, ripple drift laminations, and the pebble imbrications indicates paleoflow which matches with the modern Indus River flow. This along with the clast composition of the Indus molasses suggests it as the paleochannel of Indus River. The gravely and well stratified deposits occurring at the units 50 and 51 overlying the aeolian facies, contain eniterly of granitic clasts depicting the glacial outwash deposits from the Ladakh batholithic domain.

The elevated paleo-river channels and the sudden arrival of the lacustrine conditions at 24 m depict the raised base level most probably due to damming like effect. The downstream exit of the Leh valley is displayed by extensive moraine activity as well as moraine recycled sedimentation capable of blocking the Indus River leading to widespread lacustrine conditions. This has led to basin over fill conditions with respect to the already elevated base levels. Further, the gradual induction of aeolian conditions in the upper part of the varve facies indicates widespread increase of cold-arid conditions. The glacial outwash facies overlying the aeolian facies indicates sudden warming that followed the destruction of lake basins along with rapid incision. Continued warming resulted in recharging of the Indus River leading to the valley incision till the modern T_0 surface.

SEDIMENT SOURCE VARIATION FROM MINERAL MAGNETISM

The mass specific susceptibility (χ_{lf}) for the Spituk-Leh samples varies from 0.41 to 35 ($10e^{-8}m^3/kg$) with a mean of 8.7 and median of 3.6 suggesting weakly ferromagnetic nature of samples. The mean frequency dependence of susceptibility (χ_{fd}%) is less than 0.4% with a rare value of

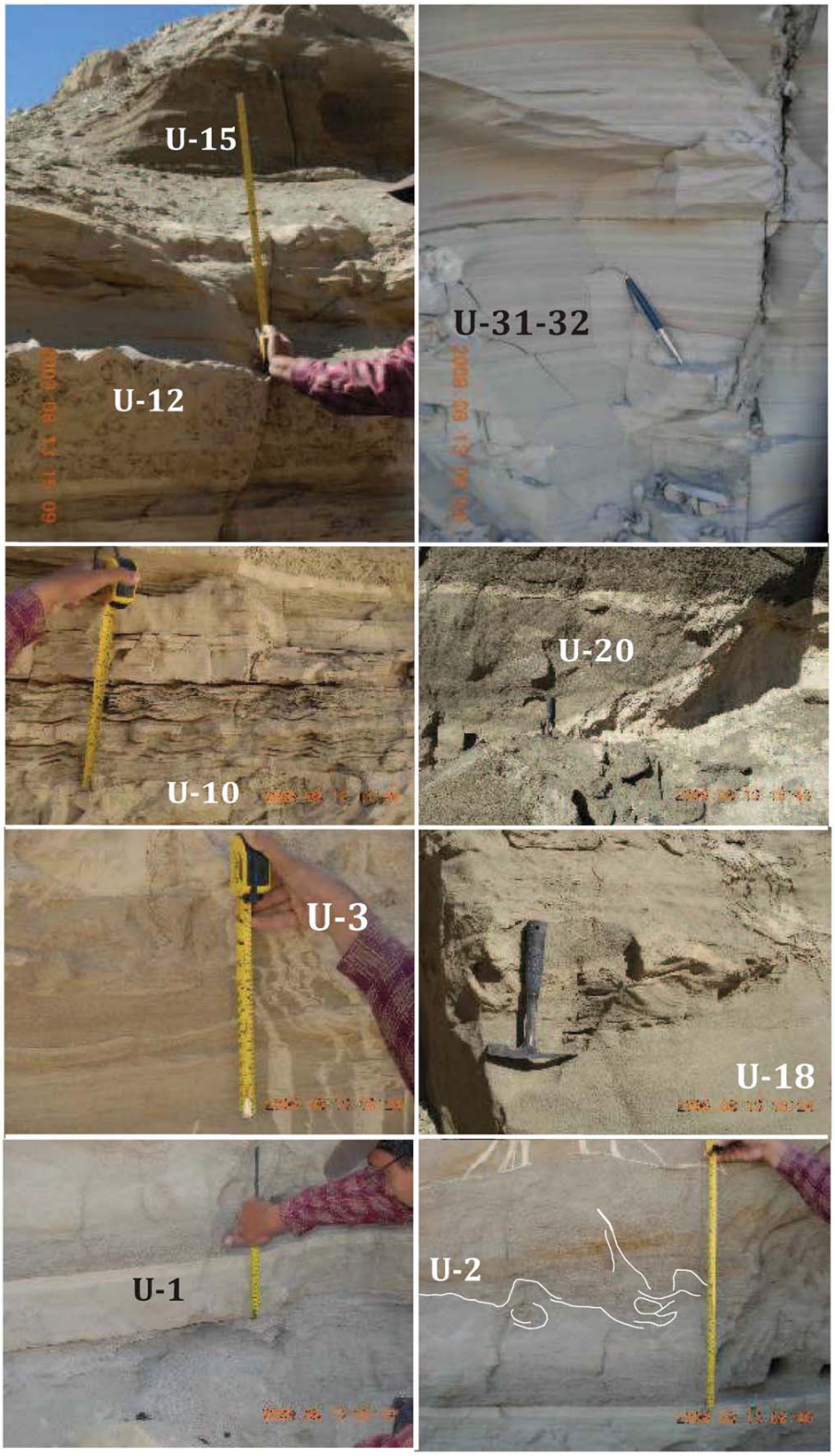

Fig.5. Some of the characteristic features of depositional environments depicting dynamic changes. *U-1*: first appearance of the lacustrine mud facies, U-2: fining upward sequence grading from grey sand to yellowish mud showing PCDs, *U-3*: lacustrine facies with PCDs, *U-10*: ripple drift laminated silt and mud layers, *U-12*: complexly laminated structures, *U-15*: fluvial excursion, *U-18*: fine to medium grained sand with cannibalized lacustrine mud, *U-20*: coarse grained grey sand of Indus affinity with high scouring and cannibalized lake beds, *U-31-32*: typical varvites.

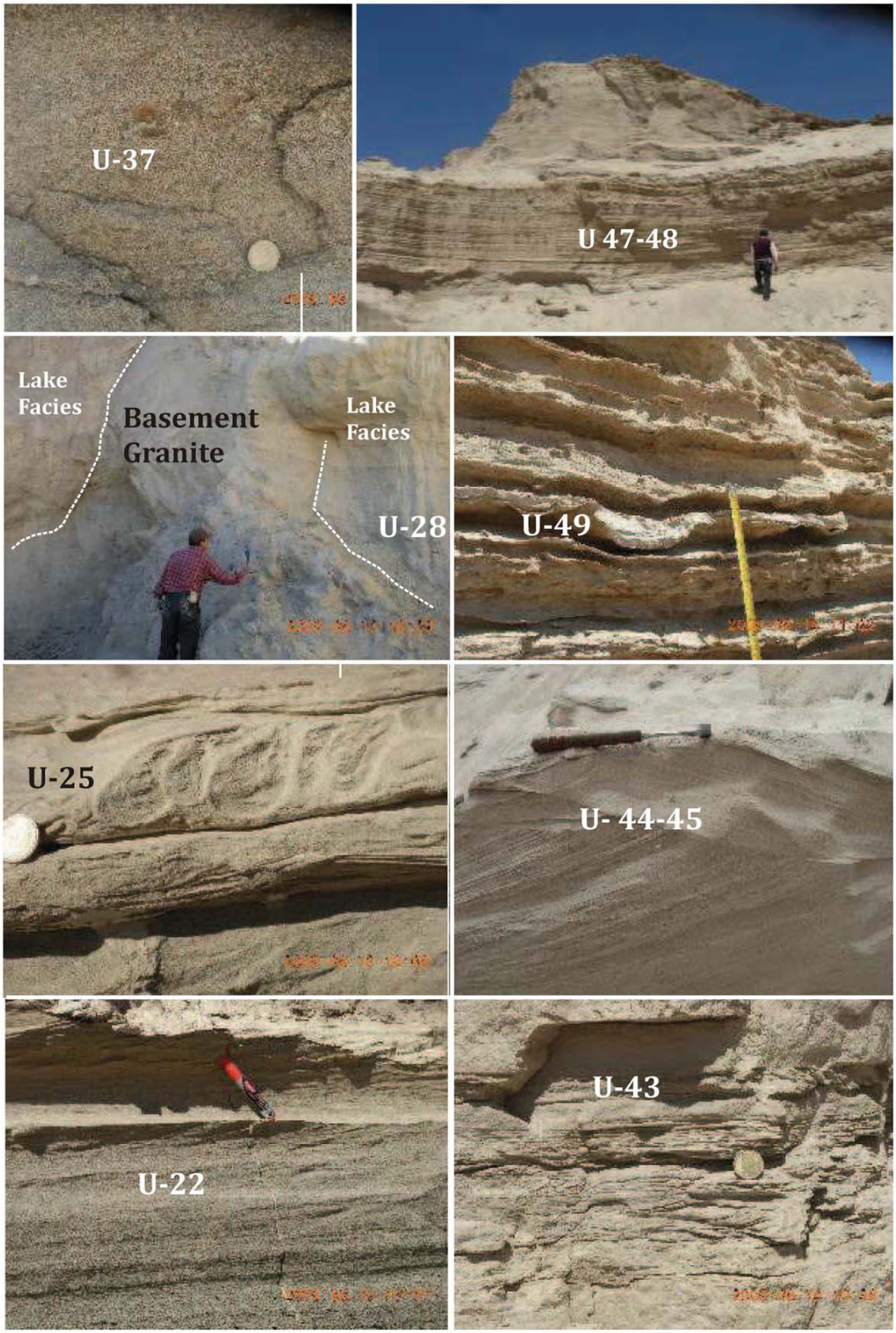

Fig.6. Some of the characteristic features depicting the varied depositional regimes in the studied profile. *U-22*: horizontally and cross bedded fining upward sands of Indus source, *U-25*: pseudo-nodules related to PCD, *U-28*: glacial horn like feature protruding from the lake basement made up of the Ladakh granodiorite, *U-37*: typical batholith sourced-, coarse grained, yellowish sand, U-43: thinly laminated silt-mud alternations, *U-44-45*: typical aeolian dune facies, *U-47-48*: larger view of the transitional, stratified outwash deposits, *U-49*: Glacial outwash deposit overlying the aeolian dune facies.

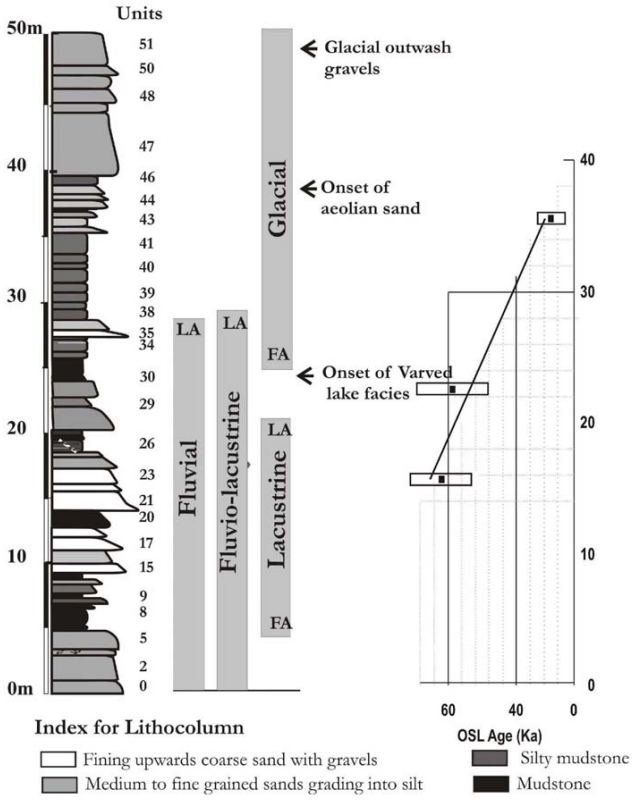

Fig.7. Compilation of the depositional environments with their first and last appearances and their correlation to interpolated/extrapolated ages derived from the best fit line of three OSL ages (the error bars are shown as rectangles).

1.4 suggesting the absence of finer/Superparamagnetic (SP) fraction which is normally observed in pedogenic environments. The S-ratio varies from -0.8 to 0 with a mean value of -0.46 suggesting predominance of Multi Domain ferrimagnets that are characteristic of detrital grains. The *Hcr* varies from 4 to 108 mT with mean as well as median of ~45 mT. The higher values of the order of 100 mT are characteristic of the presence of antiferromagnetic minerals like hematite. In detrital mineralogy these can be observed in the Indus molasse derived source and the in-situ hematite/ limonite/goethite in the lacustrine phases. Majority of the samples indicate unimodal nature of ferrimagnetic mineralogy with variation in grain size. Some samples have shown antiferromagnetic and mixed ferri- and antiferromagnetic composition.

The χ_{ARM} and χ_{lf} shows a good positive correlation (Pearson coefficient = 0.7) indicating ferrimagnetic control over susceptibility. There is significant positive correlation between χ_{lf} and $Soft_{IRM}$ (0.83) and good correlation between χ_{lf} and SIRM (0.66) attesting the ferrimagnetic control of mass specific susceptibility. Significant positive correlation is also evident amongst χ_{ARM}, SIRM and $Soft_{IRM}$. This suggests that the variation in SD concentration is proportionate to that of MD and PSD grains, and infers that all the ferrimagnetic concentration is of detrital nature. Thus the detrital modes are broadly indicative of ferrimagnetic nature for the batholithic source and the mixed ferri- to antiferromagnetic nature for the Indus molasse source.

With the routine mineral magnetic approach we have attempted to distinguish between ferrimagnetically rich granodioritic batholithic sands against the anti-ferromagnetic and mixed Indus molasses source to assign its relation with changes in depositional environments as below. It is inferred that the sediment deposition in the Leh valley basin is characteristic of two contrasting sources: (A) the Ladakh batholithic source mostly appearing as yellowish grey sands with unimodal ferrimagnetic mineralogy; and (B) the Indus molasse sedimentary source appearing as dark grey sands (e.g., seen in Figs. 4 to 6), with a mixture of ferri- and antiferromagnetic mineralogy.

MINERAL MAGNETIC RESPONSE TO DEPOSITIONAL ENVIRONMENTS

We integrate the mineral magnetic and lithologic information to infer the depositional conditions for each unit. A peak at 3.5 m level for the χ_{lf} corresponds to drop in *Hcr* and low negative S-Ratios within the yellowish grey, fining upward, medium to fine grained sands of unit 5 (Figs. 7 and 8). This suggests a detritus of overall larger ferrimagnetic grains, characteristic of the yellowish grey granite/granodioritic sands derived from the Ladakh batholith. It follows that the *Hcr* varying from 30 to 65 mT with low χ_{lf} and higher SIRM between 5 and 10m in the lithosection suggest presence of finer ferrimagnetic grains. It corresponds to the units 7 to 14 comprising of low energy conditions reflected by the deposition of massive to thinly laminated mudstones, silty mud and silt. A peak in *Hcr* (>90 mT), positive S-Ratio (~1), low χ_{lf} and low SIRM at 15 m level is shown by the typical dark grey, fining upward, coarse to medium grained sands of the Indus molasse composition. A peak in SIRM, SIRM/χ_{lf}, positive S-Ratio and high *Hcr* (~60 – 80 mT) with minor peak of χ_{lf} at ~18 m (U/25) suggests a mixed ferri to antiferromagnetic mineralogy. This unit shows mixed, dark grey to yellowish grey sands. Further upwards from 19 to 23 m interval, similar behavior in the mineral magnetic parameters (as above) but with downward trends of χ_{lf}, SIRM and SIRM/χ_{lf} suggests decreasing ferrimagnetic concentration. This interval corresponds to the mudstone dominant interval of units 26 to 31.

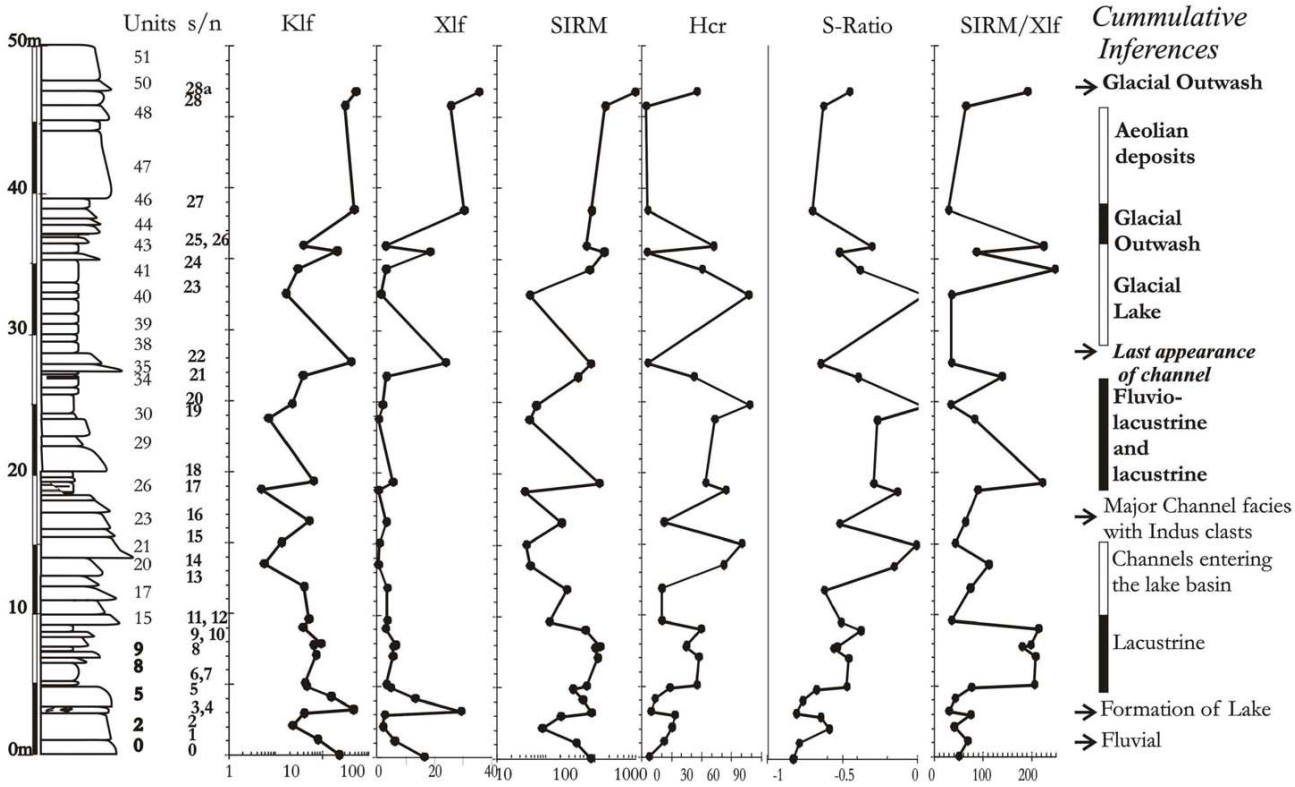

Fig.8. Variation in the mineral magnetic parameters along with the depositional environments for the studied litho-section of Spituk in the Leh valley basin.

A peak in *Hcr* at 25 m corresponds to similar peak in S-ratio, and drop in SIRM without much alteration in χ_{lf} in the units 31 to 32. This suggests the presence of antiferromagnetic mineral like hematite without any remarkable detrital influx. It follows a downward trend in *Hcr* and S-Ratios with increasing SIRM till 27 m occurring in similar manner to that of the mudstones (as above) and till unit 35. There is a great variability in varve frequency amongst these units broadly maintaining a lower frequency and hematitic (/limonitic) nature in the lower units, and higher varve frequency but less hematitic nature in the upper units. This episode, therefore, indicates a gradual climatic shift from warmer to cooler conditions. A major peak in *Hcr* and S-Ratio with low SIRM, SIRM/χ_{lf} and χ_{lf} is observed at ~32 m level (unit 40) which comprises of inter-layered mud (limonitic) and sands; suggesting warmer phase with improved seasonality. Further, there are variations within these conditions till 37 m. This follows the thick sequence of cross bedded sands till 45 m level showing low *Hcr*, negative S-Ratio and higher SIRM and χ_{lf}. Since there is no visible difference in the nature of sands, and the stratification is subdued by the large cross stratified bedding of aeolian dune nature (Fig. 6, units 44-45); we relied upon low sampling interval in this zone. The interval from 45 to 48 m further shows alternate aeolian sand and limonitic mud deposition indicating episodic cooling and warming. This is in agreement with the alternate changes in mineralogy indicated by H_{CR}, S-Ratio and SIRM/χ_{lf}.

CLIMATIC RECONSTRUCTIONS FROM THE DEPOSITIONAL ENVIRONMENTS

The first major change in depositional environments is observed at ~24 m level from the base where the lower fluvio-lacustrine conditions changed to varved lake facies. This changeover corresponds to the OSL age of 64±12 Ka. The Spituk site geographically falls in the domain of Leh stage glaciation (described in Owen et al. 2006). The above age of the studied section, therefore, can be bracketed within the 'Kar' glacial stage operated over the Ladakh batholithic domain of Leh valley (during ~100 to 60 Ka; Owen et al. 2006). The youngest (/terminal) age of the moraines near Leh (in the right bank of Indus, Owen et al. 2006) probably coincides with our above OSL age. This indicates that the varved lake facies at Spituk corresponds to the Kar stage glaciation of Owen et al. (2006).

The Phyang moraine in the downstream of the Leh valley remained active at least till 40 Ka (the youngest

TCN age of the Phyang moraine boulder, *op. cit*). This suggests that the recessional stage of the glacier, producing excessive sediment with melt waters created blockade to the Indus River raising the base levels favourable for the fluvio-lacustrine conditions in the Leh valley as documented in the Spituk section. Continuation of the lacustrine phase resulted in basin overfilled conditions and further prolonged cooling during younger glacial stages resulted in extensive aeolian phases in the valley. Finally, the Holocene warming resulted in the supply of greater moisture to the glaciers with seasonal melting to produce the glacial outwash deposits as observed in the topmost part of the Spituk section (unit 51) overlying the aeolian facies.

It appears that the basin fill conditions and the changes at base level in the Leh valley are governed by this broad climatic scenario. In the earliest phase, the collage of Indus paraglacial fans from the left bank appears to have raised the base levels during extensive Mid-Pleistocene glaciation (Jamiesson et al. 2004). These para-glacial fans have also forced the thalweg of transversely flowing Indus River towards the right bank, besides providing the recycled detritus of Indus molasses clasts. The fan sedimentation receded with the termination of the Indus glacial stage (~400 Ka, Owen et al. 2006). The Equilibrium Line Altitude (ELA) then further depressed far into the Zanskar ranges producing the melt-water valleys and trenches in the inter fan area. This is followed by the advancement of younger glacial stages operative over the Ladakah batholithic domain (Owen et al. 2006; Hobley et al. 2010). Advancement of the moraines from these Ladakh batholithic ranges resulted in their dynamic interaction with the Indus River. This is remarkably shown by moraine-scouring of the Indus alluvium in the right bank outcrops (e.g., Fig. 3a). The advancement resulted in moraine ridges damming the trunk river, while the retreat caused extensive melting producing lacustrine to fluvio- lacustrine conditions in the main valley. The damming like situation has controlled the abrupt base level changes during these (/younger) glaciation stages. Retreat of this glacial phase subsequently resulted in sediment entrapments in the transverse valleys (e.g., Hobley et al. 2010) and sculpting of the transverse amphitheater valleys (Sant et al. 2011). It appears that intensive warming during Holocene resulted in low sediment:water ratios producing conditions like breaching of lakes, valley (self-) incision and further higher sediment transport by Indus to evacuate the valley in the present form. Previously, Clift et al. (2004) linked the high sediment flux from the Indus River during the last glacial to Holocene to tectonic causes, but the present work favors the climate change as one of the major cause of sediment flux control of Indus River during Late Quaternary.

CONCLUSION

The integrated approach of lithologic documentation aided by mineral magnetism and OSL chronology reveals three stages of evolution of the Leh valley basin during Late Quaternary climatic oscillations namely: (*I)* the basin under-fill conditions marked by fluvial and fluvio-lacustrine phase till ~24 m (~64 Ka OSL age) above modern base level followed by (*II)* the predominantly varved, glacio-lacustrine and overfilled phase till 38 m (~28 Ka) gradually passing into the aeolian phase; and (*III)* basin incision that began at the earliest Holocene warming. These broad evolutionary phases are articulated by the dynamic base level changes in response to shift in climate vis-a-vis basin fill conditions. The moraines from transverse valleys appear to have greatly controlled the higher order changes in the basin fill conditions as well as depositional environments. The mineral magnetic studies have helped to trace the variability of the two contrasting sources (Indus Molasse and Ladakh batholith) depicting independent glacial domains. Similar documentation with better chronologic correlation over other exposed records within the valley would enable to reconstruct the evolution of the Leh valley basin in the context of Quaternary climatic changes.

Acknowledgements: The present work was carried out by the funding under the DST (Government of India) grant (SR/S4/ES-130/2004) to NRP, SJS and SR. We are grateful to local authorities for the necessary permission to work in this strategic area. Critical reviews and suggestions from anonymous referees have substantially improved the manuscript. We acknowledge the encouragements and necessary facilities and permissions provided by Director, Wadia Institute of Himalayan Geology (WIHG), Dehradun. Mr. Rakesh Kumar at Rock Magnetic laboratory (WIHG) is acknowledged for help during analysis.

References

BENN, D.I. and OWEN, L.A. (2002) Himalayan glacial sedimentary environments: a framework for reconstructing and dating the former extent of glaciers in high mountains. Quaternary Internat., v.97-98, pp.3-25.

BOOKHAGEN, B., RASMUS, C., THIEDE, M. and STRECKER, R. (2005) Late Quaternary intensified monsoon phases control landscape evolution in the northwest Himalaya. Geology, v.33(2), pp.149-152.

BÜRGISSER, H. M., GANSSER, A. and PIKA, J. (1982) Late Glacial lake sediments of the Indus valley area, northwestern Himalaya. Eclogae. Geol. Helv., v.75, pp.51-63.

CLIFT, P. D., CAMPBELL, I. H., PRINGLE, M. S., CARTER, A. and ZHANG, X., et al. (2004) Thermochronology of the modern Indus River bedload: New insights into the controls on the marine stratigraphic record. Tectonics, v.23, pp.1-17.

COLLINSON, D.W. (1987) Methods in Rock magnetism and palaeomagnetism: techniques and Instrumentation. Chapman and Hall Publication 503p.

DULLER, G. A.T. (2008) Luminescence Dating: guidelines on using luminescence dating in archaeology. English Heritage (Report): 45pp.

DUNLOP, D.J. and OZDEMIR, O. (1997) Rock magnetism: fundamentals and frontiers, Cambridge University Press, 573p.

EVANS, M.E. and HELLER, F. (2003) Environmental magnetism: Principles and applications of enviromagnetics, International Geophysics Series, Academic Press, no.86, 293p.

FORT, M. (1982) Geomorphological Observations in the Ladakh area (Himalaya) :Quaternary evolution and present dynamics. *In:* V.J. Gupta (Ed.), Contributions to Himalayan Geology 2, Hindustan Publ. Co., Delhi, pp.39-58.

FORT, M., BURBANK, D.W. and FREYTET, P. (1989) Lacustrine sedimentation in a semi-arid alpine setting: an example from Ladakh, northwest Himalaya. Quaternary Res., v.31/3, pp.332-350.

HOBLEY, D.E.J., SINCLAIR, H.D. and PATIENCE, A.C. (2010) Processes, rates, and time scales of fluvial response in an ancient post glacial landscape of the northwest Indian Himalaya. Geol. Soc. Am. Bull., v.122, pp.1569-1584.

JAMIESSON, S.S.R., SINCLIAR, H.D., KIRSTEIN, L.A. and PURVES, R. S. (2004) Tectonic forcing of longitudinal valleys in the Himalaya: morphological analysis of the Ladakh Batholith, North India. Geomorphology, v.58(1-4), pp.49-65.

KOTLIA, B.S., SHUKLA, U.K., BHALLA, M.S., MATHUR, P.D. and PANT, C.C. (1997) Quaternary fluvio-lacustrine deposits of Lamayuru basin, Ladakh Himalaya: preliminary palaeolake investigations. Geological Mag., v.134/6, pp.807-812.

MITCHELL, W. A., TAYLOR, P. J. and OSMASTON, H. (1999) Quaternary geology in Zanskar, NW Indian Himalaya: evidence for restricted glaciation and preglacial topography. Jour. Asian Earth Sci., v.17, pp.307-318.

MURRAY, A.S. and WINTLE, A.G. (2000) Luminescence dating of quartz using an improved single-aliquot regenerative- dose protocol. Radiation Measurements, v.32, pp.57-73.

OWEN, L.A., CAFFEE, M.W., BOVARD, K.R., FINKEL, R.C. and SHARMA, M. C. (2006) Terrestrial cosmogenic nuclide surface exposure dating of the oldest glacial successions in the Himalayan orogen: Ladakh Range, northern India. GSA Bull., no.118 ¾, pp.383-392.

OWEN, L. A., DERBYSHIRE, E. and FORT, M. (1998) The Quaternary Glacial History of the Himalaya. Quat. Proc., 6, pp.91-120.

OWEN, L.A., FINKEL, R.C., BARNARD, P. I., MA, H., ASAHI, K., CAFFEE, M.W. and DERBYSHIRE, E. (2005) Climatic and topographic controls on the style and timing of Late Quaternary glaciation throughout Tibet and the Himalaya defined by ^{10}Be cosmogenic radionuclide surface exposure dating. Quaternary Sci. Rev., v.24, pp. 1391–1411.

OWEN, L. A., THACKRAY, G., ANDERSON, R. S., BRINER, J., KAUFMAN, D., ROE, G., PFEFFER, W. and YI, C. (2009) Integrated research on mountain glaciers: Current status, priorities and future prospects. Geomorphology, v.103, pp.158-171.

PHARTIYAL B., SHARMA A., UPADHYAY R., RAM-AWATAR and SINHA A.K. (2005) Quaternary geology, tectonics and distribution of palaeo- and present fluvio/glacio lacustrine deposits in Ladakh, NW Indian Himalaya – a study based on field observations. Geomorphology, v.65, pp.241-256.

SANGODE, S.J. and BAGATI, T.N. (1995) Tectono-climatic signatures in higher Himalayan lakes: a palaeomagnetic rock magnetic approach in the lacustrine sediments of Lamayuru, Ladakh, India. Jour. Himalayan Geol., v.6, pp. 51-60.

SANGODE, S.J. and GUPTA, K.R. (2010) An Overview of two Decades of Quaternary Research in India: Some reflections based on Bibliographic Analysis. Episodes, v.33, pp.109-115.

SANGODE, S. J., PHADTARE, N. R., MESHRAM, D. C., RAWAT, S. and SURESH, N. (2011) A Record of Lake Outburst in the Indus Valley of Ladakh Himalaya, India. Curr. Sci., v.102/9, pp.1712-1718.

SANT, D.A., WADHWAN, S.K., GANJOO, R.K., BASAVAIAH, N., SUKUMARAN, P. and BHATTACHARYA, S. (2011a) Morphostratigraphy and palaeoclimate appraisal of the Leh valley, Ladakh Himalayas, India. Jour. Geol. Soc. India, v.**77**, pp. 499-510.

SANT, D.A., WADHWAN, S.K., GANJOO, R.K., BASAVAIAH, N., SUKUMARAN, P. and BHATTACHARYA, S. (2011b) Linkage of paraglacial processes from last glacial to recent inferred from Spituk sequence, Leh valley, Ladakh Himalaya. Jour. Geol. Soc. India, v.78, pp.147-156.

SHRODER, J.F. and HIGGINS, S.M. (1989) Quaternary glacial chronology and neotectonics in the Himalaya of northern Pakistan. Geol. Soc. Amer. Spec. Paper no.232, pp.275-294.

SHUKLA, U.K., KOTLIA, B.S. and MATHUR, P.D. (2002) Sedimentation pattern in a trans-Himalayan Quaternary lake at Lamayuru (Ladakh), India. Sedimentary Geol., v.148, pp.405-424.

THOMPSON, R. and OLDFIELD, F. (1986) Environmental magnetism. Allen and Unwin, London pp London, UK, 227p.

(Received: 18 February 2012; Revised form accepted: 24 July 2012)